



CHORUS

This is the accepted manuscript made available via CHORUS. The article has been published as:

Electrohydrodynamic aggregation with vertically inverted systems

Eric D. Ruud and Cari S. Dutcher

Phys. Rev. E **97**, 022614 — Published 26 February 2018

DOI: [10.1103/PhysRevE.97.022614](https://doi.org/10.1103/PhysRevE.97.022614)

Electrohydrodynamic aggregation with vertically inverted systems

*Eric D. Ruud, Cari S. Dutcher**

University of Minnesota, Twin Cities, Department of Mechanical Engineering, 111 Church Street SE, Minneapolis MN 55455

Corresponding Author

*cdutcher@umn.edu

PACS codes: 47.65.-d, 82.70.Dd

Electrohydrodynamics, 47.65.-d

Colloids, 82.70.Dd

ABSTRACT

Flow patterns surrounding particles suspended near electrodes within an electrolyte solution can be induced with an electric field due to an electrohydrodynamic (EHD) force. Depending on electrolyte, particle, and field properties, a variety of particle packing and stability states have been observed in EHD flow. In this work, we report evidence of EHD flow-induced aggregation of 2 μm sulfonated latex beads in NaCl and NaOH electrolytes solutions, in previously undocumented inverted particle-electrode orientations. Experimental conditions were chosen to

match previous work where aggregation was observed at a bottom electrode. Particles remain stable at the top electrode for times greater than 1 hour, and aggregation behavior is quantified in terms of growth rate and particle packing density and order. Similar aggregation behavior is seen at both top and bottom electrodes, with aggregate growth occurring more quickly within NaCl solutions than NaOH solutions at both the bottom and top electrode. In addition, an observed secondary location of stability for the vertical position of particles in NaOH electrolyte at the bottom electrode is not seen at the top electrode. Comparing these metrics to predictions made by a scaling model for EHD flow, particle aggregation behavior is predicted at both top and bottom electrodes, but the observed differences in aggregate packing are not. Thus, we suggest that modifications to existing models or their interpretation may be needed to predict behavior in such systems.

I. INTRODUCTION

Charged colloidal particles contained within an electrolyte solution induce secondary fluid flows in certain conditions due to the electrohydrodynamic (EHD) force. This force has been identified as the cause of fluid effects seen in experiments where particles exposed to an electric field display attractive forcing and form 2D close packed aggregates. [1–4] In electrohydrodynamics (also known as induced-charge electro-osmotic flow), [5–8] particles settled near an electrode distort the local electric field and free charge distribution, creating a tangential hydrodynamic flow profile, causing nearby particles to aggregate. [2,4,9,10] The complexity of these systems has made direct prediction of behavior difficult, and many variables affect system behavior, including field properties, electrolyte, ionic strength and particle characteristics. [7–9,11,12] In addition to 2D randomly (RCP) [7,9,11] and hexatically

(HCP) [8,12,13] close packed aggregates, particles may form 3D aggregates, [12,13] wormlike structures or chains, [7,11,12] binary superlattices [4], and rings. [12] Electrohydrodynamic flow may also be modified by altering particle morphology (to non-spherical configurations) or with non-uniform surface properties, creating unique, tunable flow patterns and particle interactions [14–16]

Experimental systems typically consist of two metallic coated electrodes separated by a nonconductive spacer, allowing for the application of an electric field. When an AC field is applied, the particles may aggregate, separate, or remain unaffected depending on the magnitude and frequency of the field, in addition to particle and solution properties. Previous work has characterized this packing and aggregation behavior through 2D particle and aggregate tracking in MATLAB and aggregate height measurement using confocal microscopy. [17–19] Aggregate packing metrics have illustrated a frequency-dependent packing behavior in NaCl electrolytes, with aggregates transitioning from a RCP to HCP state between 100-500Hz, and separation above 4000Hz. [17] Efforts to characterize this behavior in NaCl solutions by Dutcher et al. have found that as applied frequency was increased, particle diffusivity decreased, presumably due to a decrease in the magnitude of EHD flow. [17] This frequency shift also resulted in a change of aggregate height and packing state, as both aggregate height and particle separation decreased with an increase of frequency. A scaling model for EHD flow proposed by Ristenpart et al. [9] for EHD flow captures the qualitative trend of decreasing aggregate height with decreasing frequency by predicting interaction potential of particles. [17,19] This model also supports experimental results obtained when using an NaOH electrolyte, where two stable planes of particles are seen after a field is applied. [19] Frequency-dependent aggregation has been also been seen with NaOH electrolytes at one of these planes with a sufficiently low applied

frequency (~ 25 Hz), an electrolyte which previously had only displayed separation behavior. [20] In addition to electrolyte and field effects, aggregate formation and packing behavior has been shown to vary with electrolyte strength. [21]

In this paper, we further test the scaling model by varying the forces present in the model using a unique electrode orientation. We report the existence of stable EHD aggregation behavior at the top electrode of a fluid cell for particles in both NaOH and NaCl electrolytes. Experimental conditions are chosen to create aggregation behavior for both electrolytes at each electrode location - top and bottom. Aggregation behavior is captured and analyzed using quantitative metrics, and compared to a previously established scaling model's predictions. [9,17,19] Both electrolytes exhibit aggregation behavior at the top and bottom electrodes, though some differences are noted in quantitative comparisons. Bifurcation of particles into two vertical planes with an NaOH electrolyte was again observed at the bottom electrode, but not at the top electrode, consistent with the model prediction. [20]

II. EXPERIMENTAL

Experimental techniques we used were similar to methods by Ristenpart et al. for observing colloidal aggregation. [9,17–20] The experimental cell consisted of two $70 \text{ } \Omega/\text{sq}$ ITO-coated glass coverslips (SPI Supplies), separated by a nonconductive $750 \text{ } \mu\text{m}$ polydimethylsiloxane (PDMS) spacer. This spacer was cut with a biopsy punch to create a circular hole with an interior diameter of 8mm. Coverslips are first cleaned with soap and DI water using a soft bristle brush, then are placed in a slide tray and sonicated for 5 minutes in acetone. The coverslips are then rinsed with methanol, isopropyl alcohol and finally distilled water before being dried using filtered compressed air. Copper tape (0.25", Fisher Scientific) is applied to the edge of the

conductive side of each coverslip to be used as an attachment point for the function generator leads.

Solutions were added to a well formed by stacking the PDMS spacer on the conductive side of the ITO-coated coverslip. The second coverslip was then placed on the top of the filled well, enclosing the fluid with no air bubbles. This cell was attached to a microscope slide with non-conductive tape to facilitate transfer and allow for experiments in both orientations of the cell. Finally, the cell was stored for at least 2 hours to allow particles to settle at the bottom electrode.

Suspensions were created using 2 μm Sulfate Latex Beads (Life Technologies), suspended in a 1 mM NaCl or NaOH electrolyte. To remove stabilizing agents, the beads were mixed with the electrolyte in 2.5 ml centrifuge tubes, then centrifuged for 5 minutes. The liquid layer in the tube was then decanted, new electrolyte solution added, and the particles resuspended with mechanical agitation. This process was performed at least 3 times. Particle number densities in solution were controlled by using a micropipette to extract a controlled volume of particles, which was added to the electrolyte to achieve a volume fraction the order of 5×10^{-6} . To determine and reduce the effect of sodium bicarbonate formation in the 1 mM NaOH solutions, an experiment was performed with a NaOH solution prepared from distilled water that had been heated to its boiling point to remove dissolved oxygen and carbon dioxide (cooled to room temperature prior to addition of microspheres). Identical aggregation behavior was seen in this experiment to experiments performed in untreated distilled water. Zeta potential was measured using a Microtrac Stabino Particle Charge Titration Analyzer and is reported in Table I.

Particles were imaged at the bottom electrode using an Olympus IX-73 inverted microscope, with a Photron Fastcam Mini UX100 high-speed camera and at the top electrode using an Olympus BX41 upright microscope with the same camera. AC fields were applied using an Agilent 33220a function generator, set to high impedance mode. A voltage of 10 Vpp (Volts peak to peak) was applied, at a frequency of 100 Hz for NaCl and 25 Hz for NaOH to create conditions similar to those found to cause aggregation in each electrolyte. [9,20] This voltage was also chosen as particles were found to remain stable at top and bottom electrodes for periods greater than 1 hour, presumably due to a sufficiently large energy barrier from the depth of the secondary minimum as predicted in Table I and shown in Figure 4. Aggregation at the top and bottom electrode was observed separately; for experiments at the top electrode, particles were allowed to settle to the bottom electrode as normal, but were flipped immediately prior to experiment and field application. Particles near the top electrode were then held in place by EHD effects, while particles further from the electrode settled to the bottom of the cell.

Two types of experiments were performed to determine the aggregation rate of the system and aggregate packing behavior. Aggregate rate was measured with a 20x optical objective, achieving a 2 pixel per micrometer resolution at a framerate of 50 fps. Particles were imaged for 10 seconds without any electric field, then the field was applied and aggregation observed for 2 minutes. Aggregate packing state was measured using a 60x optical objective, achieving a 6 pixel per micron resolution at 4000 fps.

Image analysis on videos was then performed using MATLAB similar to techniques used by Dutcher et al. [17] Thresholding was used to detect particles and clusters in each image. Objects detected by the program that were smaller than a single particle were ignored as error.

The normalized rate of loss of singlets, k_E was calculated using the expression from Ristenpart et al.;

$$\frac{n_1^0}{n_1} = 1 + k_E n_1^0 t$$

Where n_1^0 is the initial particle concentration, n_1 is the particle concentration at time t , and k_E is the normalized rate of loss of singlets [9]. k_E was calculated from concentration data using a linear fit for the initial period of singlet loss, which is dominated by singlet-singlet events due to doublet formation. Rates were calculated from at least three experiments per condition. Packing state was measured using similar techniques to detect particles, then performing a Delaunay Triangulation to create distance and angular data for determining particle spacing and order. For both electrolytes and electrodes, the particle spacing and order parameter were found to not depend on aggregate size

III. RESULTS AND DISCUSSION

Colloidal aggregation behavior was observed at both top and bottom electrodes within NaCl and NaOH electrolyte systems. Experiments were performed to compare differences in kinetics and equilibrium behavior for both electrode orientations in order to explore previously unreported aggregation at the top electrode. Figure 1 shows microscopy images captured during aggregation rate experiments for all conditions. Upon application of the 100 Hz, 6.67kV/m field at $t=10$ s, particles in NaCl quickly form large clusters. Aggregates at the bottom electrode appear larger than those at the top electrode in this sample; however, this is partially due to the difficulty in retaining particles near the top electrode before field application, resulting in an effective lower particle density at the electrode. In addition, particles in 1 mM NaOH electrolyte

form smaller aggregates upon application of the 25 Hz, 6.67 kV/m field (chosen because of the aggregation behavior present at this frequency [19,20]). While particle densities of the prepared solution were similar to NaCl experiments, the bifurcation behavior of NaOH electrolytes causes a lower apparent density on the aggregation plane. As shown in Figure 2, this bifurcation behavior produces a stable, secondary layer of particles at the bottom electrode, but is unstable at the top electrode, causing bifurcated particles to settle to the bottom of the cell. Considering this behavior's effect on particle density near the electrode, aggregates in the NaOH solution appear smaller on average than those formed in NaCl, but further quantification is needed.

Particles in NaOH solutions were observed to form HCP aggregates upon application of the field while those in NaCl solutions formed RCP aggregates. These packing states were consistent for both electrode orientations. This packing behavior can be seen in the microscopy images of Figure 3 (a-d), and is quantified using particle mean spacing and particle order parameters displayed in Figure 3 (e). Work by Dutcher et al. has demonstrated a link between aggregate height and packing state, with particles further from the electrode exhibiting more tightly packed configurations before beginning to separate. [17] The observed difference in packing state between NaOH and NaCl immersed aggregates can be explained by the increased zeta potential and repulsion of the particles within NaOH solution, matching observations of Woehl et al. [18] Particle orientational bond order, Ψ_6 , is calculated using a standard orientational bond order parameter, matching the order parameter reported by Dutcher et al. While we observed aggregates retaining the same general packing state, we can see in Figure 3 (e) a difference in particle spacing when comparing aggregates at the top and bottom electrode. In general, and especially within NaCl, aggregates are more tightly packed (smaller mean spacing) and more ordered (higher Ψ_6) at the bottom electrode. From Table I and Figure 4, we

see that this behavior arose despite similar vertical locations of their secondary potential minimum, which accompanied changes in packing behavior in previous experiments at the bottom electrode. [17] Notably, aggregates at both the top and bottom electrode remained stable for more than 1 hour.

A rate constant describing singlet loss, k_E , is calculated from the normalized slope of inverse singlet concentration for all systems after the field is applied. Due to the bifurcation and slower aggregation rate in NaOH, aggregation rates were analyzed after initial separation and at $\sim t = 20$ s, while the rate of aggregation in NaCl was analyzed from $t = 10$ s after field application. Results reported in Table 1 are the average of all experiments. Notably, when comparing electrolytes at the same electrode location, NaCl exhibits faster aggregation rates than NaOH, consistent with previous experiments [18], and rates are faster for both electrolytes at the bottom electrode.

Ristenpart et al. analyzed the various forces present in colloidal interactions within an electrohydrodynamic field to create a scaling model which may be used to predict particle packing and aggregation. [9] The point-dipole model estimates electrical body force created as free charge on the electrode is influenced by the tangential component of the particle's dipole field. The strength of the dipole field is estimated using the Hinch model as derived for low-frequency fields. [22] Other colloidal-scale forces such as double-layer, van-der-Waals and gravitational force may also be modeled using appropriate colloidal or general equations as detailed by Woehl et al. [18] The model has been used in similar work to predict changes in particle packing state with variations in field [17], explain variations seen with different electrolytes, [18] and to explain bifurcations in the height of particle populations. [19] The

parameters used in the model to match the experiments in this work are detailed in Table I, and the contribution of each potential is shown in Figure 4.

The total potential as shown in Figure 4 plots the relative net strength of forces at increasing separation distances from the electrode. The location of local minimums in Figure 4 represent areas of particle stability, while the difference between the minimum and neighboring maximum represents an “energy barrier”, a measure of particle stability at these locations. All plots show a primary minimum at the wall, a secondary potential minimum at 80-90 nm (see Table I), while only NaOH exhibits an additional tertiary potential minimum (Fig. 4a). This tertiary minimum is seen in experiment as a bifurcation in particle height with NaOH, documented by Woehl et al. [19] and also in our experiments through z-scans of the settled particles (Figure 2). Notably, we only observe a single layer of stable particles within NaOH electrode at the top layer, which matches the model’s prediction of a loss of tertiary minimum when orientation is reversed as seen in Figure 4(b). However, the predicted minimum location is similar for both electrolytes at the top and bottom electrode due to the weak influence of gravitational force near to the electrode, which does not predict the change in aggregate behavior between electrodes seen in Figures 1 and 3. Minimum depth is calculated as the potential difference between the local potential minimum and the height of the closest peak, as seen in Figure 4 and quantified in Table I. Minimums calculated for the top electrode using our method predict an increase of depth by $\sim 0.2 k_b T$ at the bottom electrode, suggesting increased stability and more rapid packing. However, this also does not match the observed increases in aggregation rate at the top electrode (Table I). These observations suggest that while the model does successfully predict the existence of particle stability planes, it does not fully capture the aggregate behavior.

IV. CONCLUSIONS

We have observed EHD-induced aggregation of particles at both the top and bottom electrodes of systems with both NaCl and NaOH electrolytes. With both electrolytes, and at both electrodes, particles were stable as aggregates for $t > 1$ hr, a condition previously undocumented at the top electrode with these conditions. Applying a scaling model developed by Ristenpart et al. [9], we examine behaviors previously demonstrated and modeled in particle packing states, locations for stability and aggregation rate. [17–19] Comparing this model to experiment, we successfully predict the loss of a tertiary minimum at the top electrode with NaOH electrolyte, but do not predict experimentally observed differences in aggregate packing from this model's aggregate height prediction. Thus, we confirm that this model is successful at predicting general aggregation behavior, but the model fails to capture more nuanced differences in packing behavior due to the reversal of the gravitational force.

ACKNOWLEDGMENTS

This work was supported primarily by the National Science Foundation through the University of Minnesota MRSEC under Award Number DMR-1420013. C. S. Dutcher received support from the 3M Non-Tenured Faculty Award.

REFERENCES

- [1] Böhmer, *Langmuir* **12**, 5747 (1996).
- [2] M. Trau, D. A. Saville, and I. A. Aksay, *Science* **272**, 706 (1996).
- [3] S.-R. Yeh, M. Seul, and B. I. Shraiman, *Nature* **386**, 57 (1997).
- [4] W. D. Ristenpart, I. A. Aksay, and D. A. Saville, *Phys. Rev. Lett.* **90**, 128303 (2003).
- [5] M. Z. Bazant and T. M. Squires, *Phys. Rev. Lett.* **92**, 066101 (2004).
- [6] J. A. Fagan, P. J. Sides, and D. C. Prieve, *Langmuir* **21**, 1784 (2005).
- [7] J. D. Hoggard, P. J. Sides, and D. C. Prieve, *Langmuir* **24**, 2977 (2008).
- [8] D. C. Prieve, P. J. Sides, and C. L. Wirth, *Curr. Opin. Colloid Interface Sci.* **15**, 160 (2010).
- [9] W. D. Ristenpart, I. A. Aksay, and D. A. Saville, *Phys. Rev. E* **69**, 021405 (2004).
- [10] M. Trau, D. A. Saville, and I. A. Aksay, *Langmuir* **13**, 6375 (1997).
- [11] T. Gong, D. T. Wu, and D. W. M. Marr, *Langmuir* **18**, 10064 (2002).
- [12] K.-Q. Zhang and X. Y. Liu, *J. Chem. Phys.* **130**, 184901 (2009).
- [13] T. Gong and D. W. M. Marr, *Langmuir* **17**, 2301 (2001).
- [14] A. Boymelgreen and G. Yossifon, *Langmuir* **31**, 8243 (2015).
- [15] M. Ouriemi and P. M. Vlahovska, *Langmuir* **31**, 6298 (2015).
- [16] F. Ma, S. Wang, H. Zhao, D. T. Wu, and N. Wu, *Soft Matter* **10**, 8349 (2014).
- [17] C. S. Dutcher, T. J. Woehl, N. H. Talken, and W. D. Ristenpart, *Phys. Rev. Lett.* **111**, 128302 (2013).
- [18] T. J. Woehl, K. L. Heatley, C. S. Dutcher, N. H. Talken, and W. D. Ristenpart, *Langmuir* **30**, 4887 (2014).
- [19] T. J. Woehl, B. J. Chen, K. L. Heatley, N. H. Talken, S. C. Bukosky, C. S. Dutcher, and W. D. Ristenpart, *Phys. Rev. X* **5**, 011023 (2015).
- [20] S. C. Bukosky and W. D. Ristenpart, *Langmuir ACS J. Surf. Colloids* **31**, 9742 (2015).
- [21] S. Saini, S. C. Bukosky, and W. D. Ristenpart, *Langmuir* **32**, 4210 (2016).
- [22] E. J. Hinch, J. D. Sherwood, W. C. Chew, and P. N. Sen, *J. Chem. Soc. Faraday Trans. 2* **80**, 535 (1984).

FIGURES

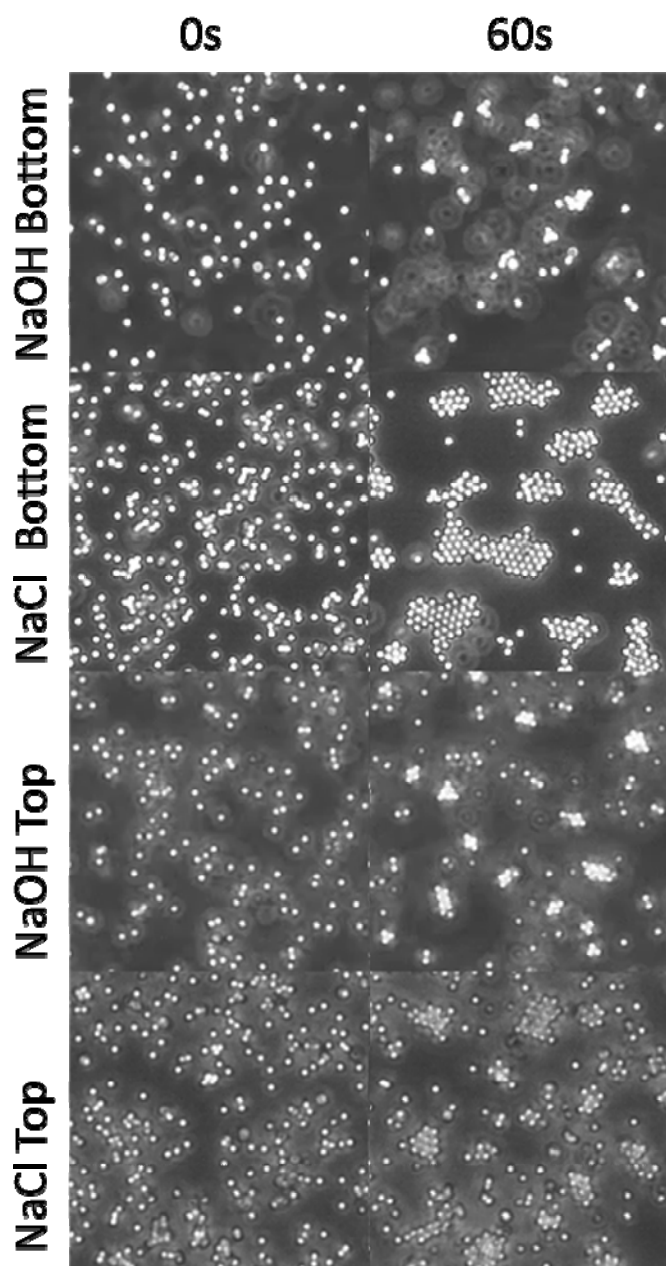


FIG. 1. Microscopy image of aggregation in NaCl and NaOH solutions at 6.67 kV/m and 100 or 25Hz, respectively. Images captured using phase contrast microscopy and a 20x objective. Particles are allowed to settle near the electrode, then are imaged for 80s with the field applied at 10s.

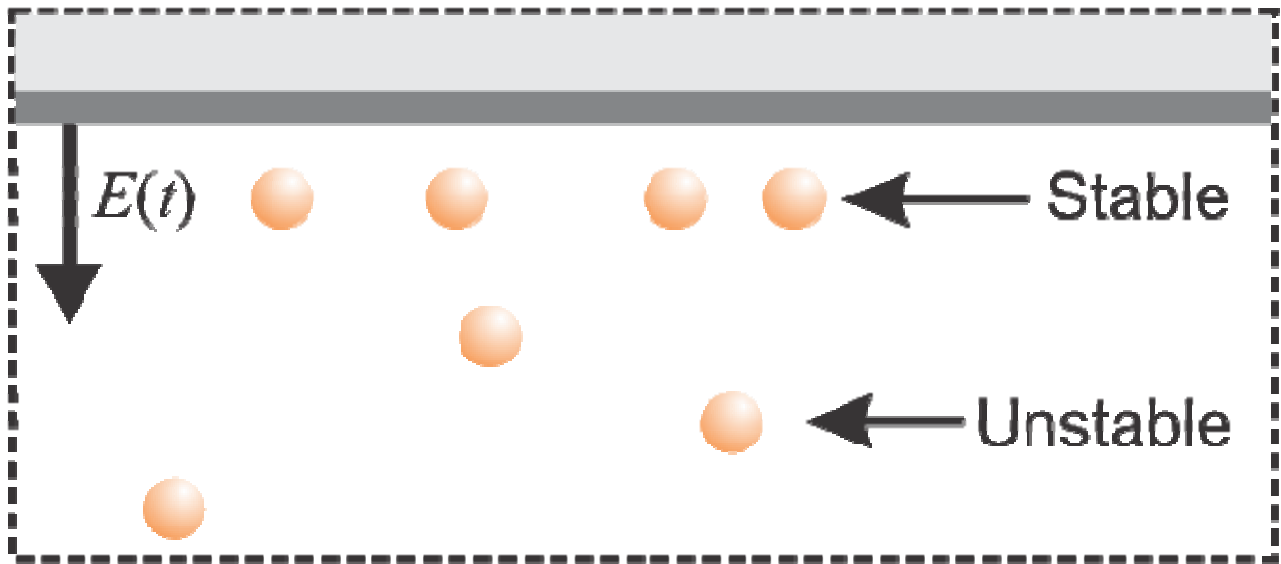


FIG. 2. Schematic of particle stability location at top electrode with a 1mM NaOH electrolyte and 25 Hz, 6.67 kV/m field magnitude. Some particles are held in place by EHD forces, while particles further from the electrode (either due to incomplete settling or bifurcation) are unstable and settle to the bottom electrode, in contrast with behavior at the bottom electrode for this system, where two planes of stability are observed.

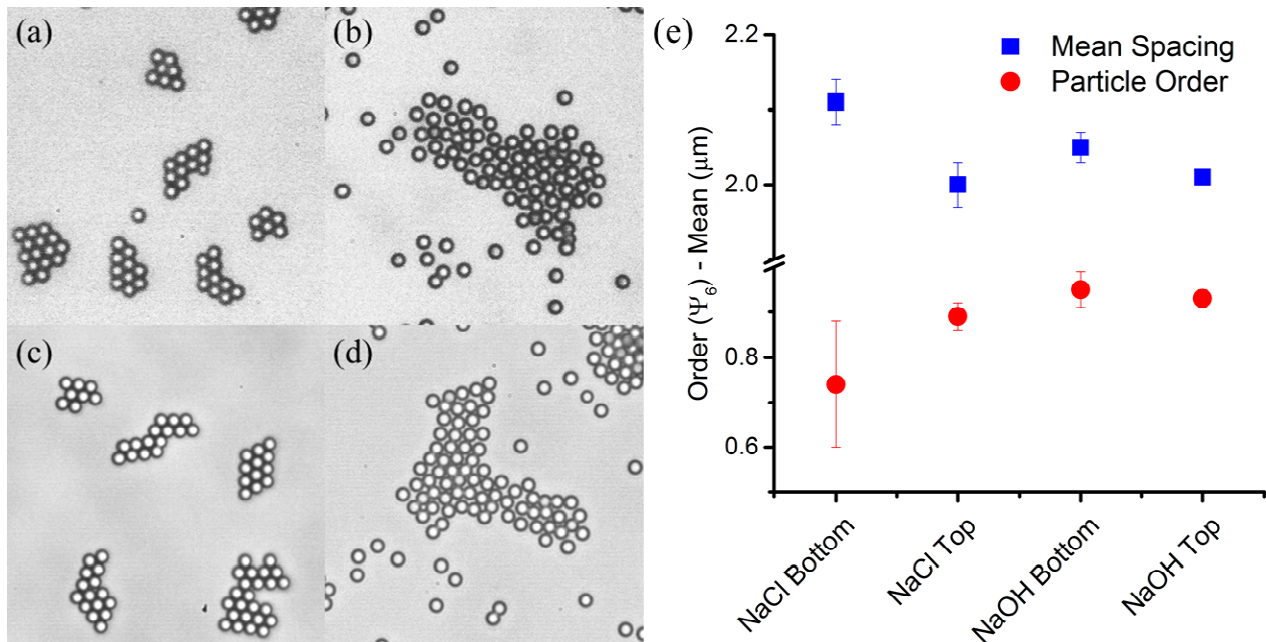


FIG. 3. Aggregates observed near electrode for normal (c,d) and inverted (a,b) orientations, within 1mM NaCl (b,d) and NaOH (a,c) electrolytes and an applied field of 10 vPP, 100Hz (NaCl) and 25Hz (NaOH) with electrode separation of 750 μm . Aggregate packing is quantified with particle spacing and order parameters (e), where a lower order parameter and higher spacing corresponds to a randomly packed aggregate (RCP), and higher order parameter and smaller mean separation corresponds to hexatic close packed (HCP) aggregates. Data represents an average of spacing and order calculations for at least 15 aggregates at each condition, measured over 4,360 frames taken at 4,000 fps after aggregates had formed.

TABLE

		Spacing (μm)	Order (Ψ_6)	2 nd Min Position (nm)	2 nd Min Depth ($k_B T$)	Aggregation Rate, k_E ($\mu\text{m}^2/\text{s}$)	Zeta Potential (mV)	Frequency (Hz)
NaCl	Bottom	$2.11 \pm .03$	$0.74 \pm .14$	81.64	1.961	24.2 ± 8.33	-58.38	100
	Top	$2.00 \pm .03$	$0.89 \pm .03$	81.88	1.734	4.21 ± 1.66	-58.38	100
NaOH	Bottom	$2.05 \pm .02$	$0.95 \pm .04$	88.32	1.949	6.75 ± 3.78	-120.0	25.0
	Top	$2.01 \pm .01$	$0.93 \pm .02$	88.58	1.720	2.38 ± 0.905	-120.0	25.0

TABLE I. Experimental conditions and results for trials. All experiments were conducted with an applied voltage of 10 Vpp, electrolyte concentration of 1 mM, EHD model fitting parameter $b=3\mu\text{m}$ (defined as lateral distance from center of particle where force is measured), and spacer thickness of 750 μm . To determine the “depth” of the secondary minimum at the “top” electrode, the difference between the secondary (2nd) minimum and local maximum furthest from the electrode was calculated. The density of the polystyrene beads is taken as 1050 kg/m^3 and the density of the dilute electrolyte solution is taken as 999.97 kg/m^3 for purposes of the model. To calculate a comparison of this value at the bottom electrode where gravitational potential prevents the formation of a similar local maximum, the location of the maximum at the top electrode was used as the x-location of a “maximum” at the bottom electrode. All potentials are scaled by thermal potential $k_B T$.

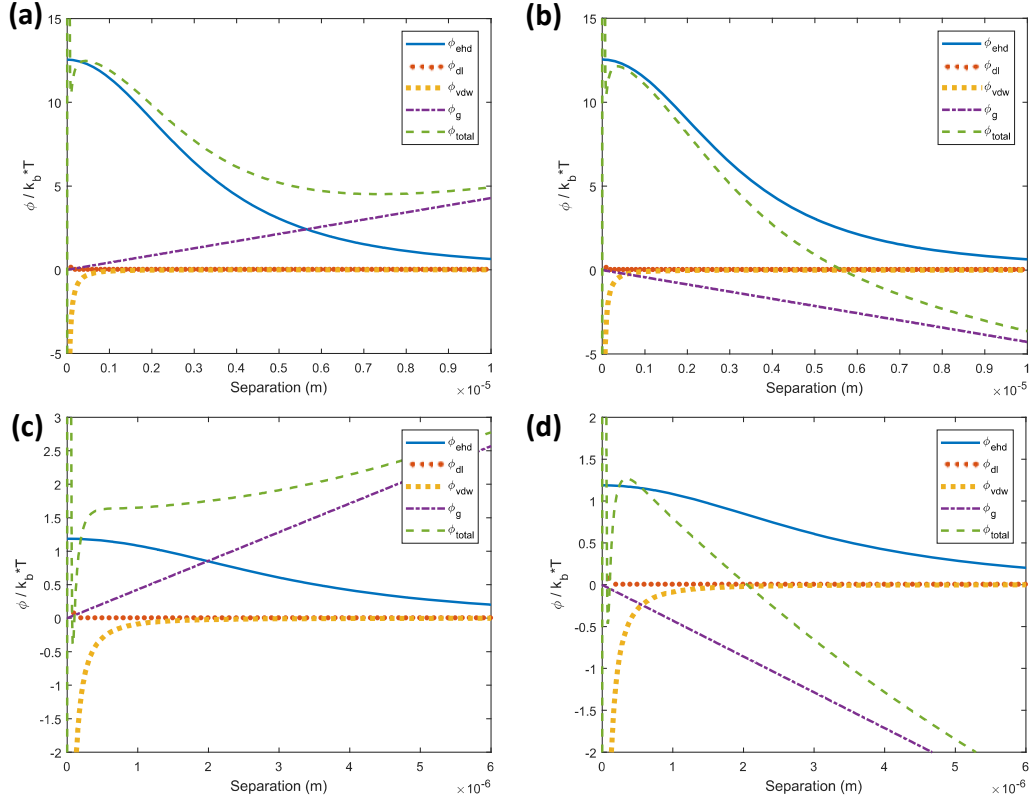


FIG. 4. Potential distribution plots for particles in NaOH (a,b) and NaCl (c,d) electrolytes at bottom (a,c) and top (b,d) electrodes. Potential is calculated for electrohydrodynamic (solid line, ehd), double-layer (dotted circles, dl), van-der-Waals (dotted squares, vdw) and gravitational forces (dash-dot, g). The total potential represents the sum of all forces (dash, total). Electrohydrodynamic potential is calculated based on the model by Ristenpart et al. [9] Separation represents the distance of the particle from the electrode. Model parameters are detailed in Table I. All potentials are scaled by thermal potential $k_B T$.